DEVELOPING A TECHNOLOGY FOR PRODUCING DRONE-BORNE HYPERSPECTRAL IMAGES TO MONITOR LARGE-AREA MIXED HERITAGE

S. H. Kim[1], J. Y. Lee[2*], K. H. Choi[3], S.J.Choi[4]

[1] Graduate School of Cultural Heritage, Korea National University of Cultural Heritage, South Korea - 20222032@nuch.ac.kr
[2] Korea National University of Cultural Heritage, South Korea - leejaeyong82@nuch.ac.kr
[3] Hyperspectral Strategic Team, GEOSTORY Co. Ltd, South Korea - jakdol@geostory.co.kr
[4] Graduate School of Cultural Heritage, Korea National University of Cultural Heritage, South Korea - 20222103@nuch.ac.kr

KEY WORDS: Heritage Preservation, Heritage Risk Assessment, Heritage Document, Natural Heritage Management, Remote Sensing,

ABSTRACT:

This study compared differences in the shooting and pre-processing techniques between manned and unmanned aerial images, and verified the precision of the images by comparing the ground sample distance between them.
GSD of manned aerial image taken at high altitude could not discern tree shapes from 150 cm per pixel, but unmanned aerial image taken at low altitude (200 m) could distinguish trees individually with 30 cm per pixel. It, therefore, found that it is efficient and economically effective to produce unmanned hyperspectral images within the large-area mixed heritage. In addition, the unmanned aerial images have lower atmospheric errors and the ground sample distance that is high enough to distinguish individual trees, so they were found to be applied to the monitoring and the diagnosis for understanding the vegetation management and the health of the large-area mixed heritage.

1. INTRODUCTION

It takes a lot of money and labor to monitor and diagnose the large-area mixed heritage, because of its large area. The monitoring and diagnosis of the ground including places which cannot be easily accessed due to their size or topological characteristics face some difficulties(Park, 2011). To resolve the problem, the use of UAV have been drastically increased since some years ago. In particular, there have been many studies on the shape recording, monitoring and diagnosis by using cameras attached to UAV and building 3D model of the heritage(Kolokoussis et al., 2021). The 3D shape model can identify the structural changes of the cultural heritage, including displacement, behavior, etc., but has difficulty in recording and diagnosing the stage of the natural heritage.

The hyperspectral image analysis using the spectral reflection of objects can be a new alternative, given the specialty of such natural heritage. In particular, it is effective in the mixed heritage combining cultural and natural heritage. It would be possible to monitor and diagnose the large-area mixed heritage distributed across a wide area, if high resolution hyperspectral images shot by UAV are made into a map by pixelating them. In addition, it is also possible to frequently and preemptively detect the occurrence and the extension of hazard factors damaging historical architectures or natural objects, which constitute the mixed heritage. This study, therefore, aims to examine the effectiveness of the aerial hyperspectral images in managing the large-area mixed heritage, by comparing differences in the production methods and the precision of images produced between manned and unmanned aerial hyperspectral images.

2. STUDY SITE AND PROCESS

2.1 Study Site and Periods

This study examined Busosanseong Fortress (about 51.6㎢) located at Buyeo, which was constructed at about the 6th century(Figure 1). Historical buildings are paced within the fortress, and various kinds of trees are raised. The field investigations into it were conducted and the data of it were also collected by using a MAV six times and UAV six times in Jun., 2021.
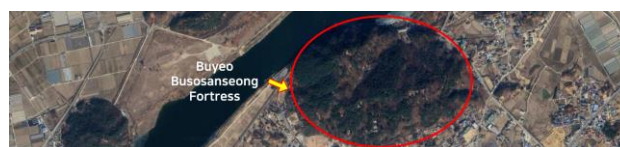

Figure 1. Position of Busosanseong Fortress

2.2 Research Equipment

This study used King Air E90 and AisaFENIX 1K for the manned aerial shooting and Matrice 300 RTK and MicroHSI Shark 410 for the unmanned aerial shooting (Table 1). It used a specific bracket directly manufactured by the researchers, to compensate the positional displacement of hyperspectral sensors, caused by wind, for the unmanned aerial shooting (Figure 2).

The International Archives of the Photogrammetry, Remote Sensing and Spatial Information Sciences, Volume XLVIII-M-2-2023
29th CIPA Symposium "Documenting, Understanding, Preserving Cultural Heritage:
Humanities and Digital Technologies for Shaping the Future", 25–30 June 2023, Florence, Italy

Category	Manned Aerial Vehicle	Unmanned Aerial Vehicle
Ground sample distance	1,024Pixel	704Pixel
Spectral Range	400~2,500 ㎚	400~1,000 ㎚
Sensor Weight	15kg	0.68kg
Hyper spectral Sensor	AisaFENIX 1K	MicroHSI Shark 410
Vehicle	King Air E90	Matrice 300RTK

Table 1. Kinds and Specifications of Research Equipment

Figure 2. Bracket for UAV

2.3 Study Process

The study process largely consists of three steps: the acquisition of hyperspectral images, the pre-processing of the hyperspectral images acquired and the verification of the precision. First, it acquired the images by MAV and UAV (Figure 3). It implemented the calibration for minimizing the positional error in acquiring images, and attempted to acquire the homogeneous spectral data, by preplanning the aerial altitude, direction and time. Second, it made the images acquired subject to the radiometric/geometric/atmospheric correction, and this study converted many images into a mosaic image. Then, it removed noises. It also made the images subject the inspection to keep the quality of them at all pre-processing steps. Third, it examined whether the images can be applied to the monitoring and the diagnosis of the large-area mixed and the natural heritage, by reviewing the precision of them to verify whether the trees appearing in them can be distinguished.
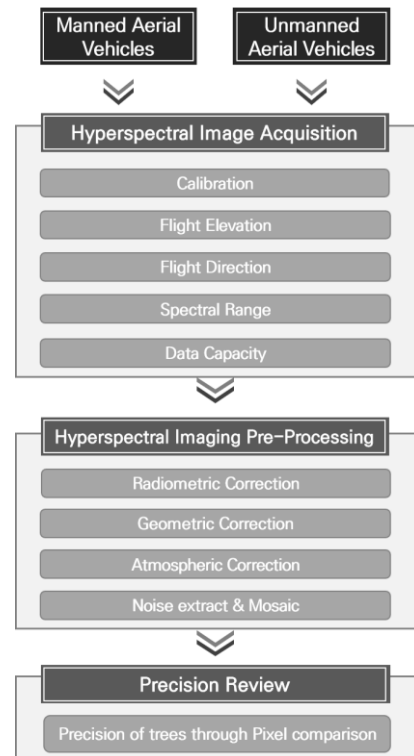

Figure 3. Study Flow Diagram

2.4 Acquisition of Hyperspectral Images

This study examined the spatial composition, topography, etc. by conducting a field investigation into the site, and therefore, made a plan for shooting it by using MAV and UAV. It performed the Boresight Calibration, to compensate the difference in the rotation and positional errors, caused by the space between the hyperspectral sensors and GPS/INS, after the vehicles were equipped with the sensors(Park et al., 2021). It compensated the geometric errors, based on paving boundaries, outlines of buildings, etc. in the site.

At the high altitude, MAV shoots the site in the ground sample distance lower than that of UAV, so this study repeatedly performed the Boresight Calibration by dividing it into three courses, until the geometric errors did not occur(Figure 4). On the other hand, UAV shoots it in the high ground sample distance at the low altitude, so the Boresight Calibration was once performed.
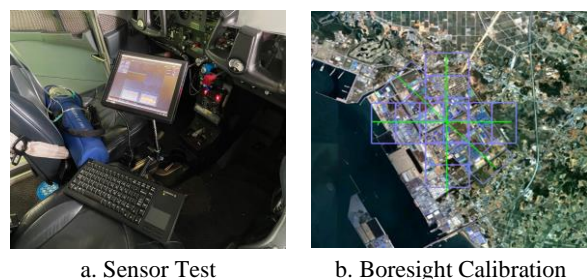

a. Sensor Test   b. Boresight Calibration
Figure 4. MAV Calibration

It performed the GPS sensor calibration only for the hyperspectral sensors applied to drones. It would not be possible to acquire accurate positional information, because errors occur in the positional information acquired from the GPS sensors, though the site can be shot by hyperspectral sensors, if drone-borne hyperspectral images are shot without the GPS sensor

The International Archives of the Photogrammetry, Remote Sensing and Spatial Information Sciences, Volume XLVIII-M-2-2023
29th CIPA Symposium "Documenting, Understanding, Preserving Cultural Heritage:
Humanities and Digital Technologies for Shaping the Future", 25–30 June 2023, Florence, Italy

calibration. The unmanned aerial photograph performed the GPS sensor calibration, through forward, backward and high-speed movement and the flight in the shape of ∞, to acquire accurate positional information(figure 5).


Figure 5. Unmanned Aerial Vehicle Sensor Calibration

It set the shooting time as noon in which the sun altitude angle is maintained, to minimize the deviation of the spectral data among the courses. It performed both the bi-direction and the uni-direction flight, which are generally conducted for the MAV's and UAV's image shooting(Figure 6). It is easy to join many images acquired from the uni-direction flight, because the shadows of objects are consistently shot in a uni-direction. Meanwhile, it used the images acquired from the bi-direction shooting as the reference data for verifying the spectral data information and errors between both images acquired.

The hyperspectral sensors belong to the push broom type, so the more the shooting overlap, the more the side overlap, for the MAV. It, therefore, reduced the flight speed to 40 ㎧, since the rotation frequency of each drone increased, due to the shorter distance among the courses. UAV shoots the images at the low altitude, so it is very important to keep the same sun altitude angle. It, therefore, allowed the range of a single flight to include a course, among many divided ones, during the shooting, and set the overlap as at least more than 65%, and the flying speed as 10 ㎧.
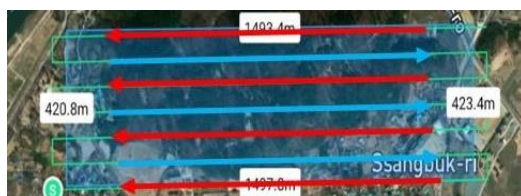
a. uni-direction

b. bi-direction

Figure 6. Photography Direction and Overlapping Test of UAV

The acquisition outcomes indicate that MAV has limits in the procedures for taking off and landing at a designated place, due to its size and stability problem. It was easy to shoot the large area, as it flew at the altitude higher than 2,000m, in acquiring data. It, however, has lower ground sample distance and was greatly influenced by the atmospheric errors caused by clouds. Although the hyperspectral sensors applied to MAV have the

bandwidth wider than those of UAV, their processing speed is lower, because the increase of their data capacity.

On the contrary, UAV can freely take off or land at any places and has advantages in shooting at the low latitude, compared to MAV. The images acquired have fewer atmospheric errors, so they have high ground sample space. The hyperspectral sensors applied to it acquire the waves ranging from 400 to 1,000nm and has the data capacity of 1-2GB, which is much less than that of MAV, so its processing speed was very fast. There were also differences in the labor and money taken to operate between UAV and MAV(Table 2).

Cate\gory	Manned Aerial Vehicle	Unmanned Aerial Vehicle
Shooting Altitude	High Altitude (higher than 2,000m)	Low Altitude (100-250m)
Shooting Area	Wide	Narrow
Place for Taking Off and Landing	Limited to Airports	Freely Selected
Error	Greatly Influenced by Atmospheric Error	Slightly Influenced by Atmospheric Error
Data Capacity	About 30GB	About 1-2GB
Processing Speed	Slow	Fast
Bandwidth	400-2,500 ㎚	400-1,500 ㎚
Shooting Cost	Expensive	Inexpensive
Labor	Four Persons	Three Persons

Table 2. Comparison of Hyperspectral Shooting between MAV and UAV

2.5 Pre-processing of Hyperspectral Images

The pre-processing process of MAV-borne hyperspectral images is conducted by the Boresight Calibration, followed by the radiometric correction, and then, the geometric correction, the atmospheric correction, the removal of noises and the Making a Mosaic of images, while that of UAV-borne hyperspectral images is conducted by radiometric correction, followed by the geometric correction, and then, the Mosaic and the atmospheric correction.

2.5.1 Boresight Calibration: It is only conducted at the pre-processing of MAV-borne hyperspectral images, which is a part of the Boresight Calibration conducted in acquiring images. This study corrected the errors in the MAV-borne hyperspectral images acquired from three courses, by designating 10-11 tie points by the courses(Figure 7).

It performed the Boresight Calibration before the radiometric and geometric correction, and used the resulting values for them. The geometric errors would occur, if the Boresight Calibration is not performed, so it is an essential process for the MAV-borne hyperspectral images.
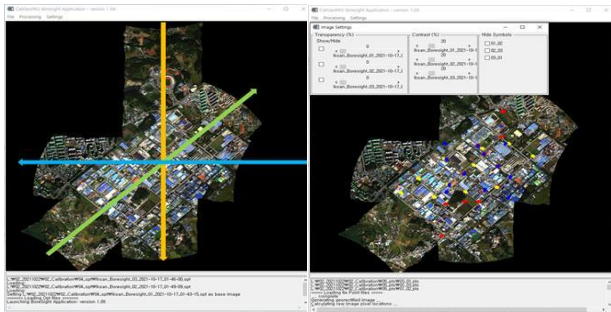
The International Archives of the Photogrammetry, Remote Sensing and Spatial Information Sciences, Volume XLVIII-M-2-2023
29th CIPA Symposium "Documenting, Understanding, Preserving Cultural Heritage:
Humanities and Digital Technologies for Shaping the Future", 25–30 June 2023, Florence, Italy

Figure 7. Manned Aerial Vehicle Sensor Calibration

2.5.2   Radiometric Correction: The radiometric correction is a technique for correcting the radiometric value distortion caused by the geometric relation between the energy radiated from the earth's surface and the detector, and the detector's response characteristics(Park, 2011). It undergoes the process for calculating the normalized radiance from the hyperspectral images consisting of the unitless digital number(DN) (Jensen, 2016). This study corrected the manned aerial hyperspectral images, by inputting the Radiometric Calibration data. It verified the correction results, by comparing the data before and after the correction. Then, it was found that the data values were corrected, as the original data values ranged from 0 to 30,000%, while the data values after correction ranged from 0 to 7,000%(Figure 8).
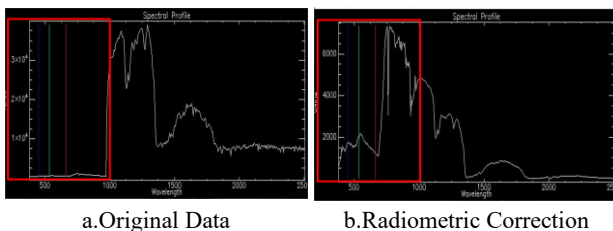

a.Original Data   b.Radiometric Correction

Figure 8. Calibration Results of Manned Aerial Hyperspectral

It performed the radiometric correction for the unmanned aerial hyperspectral images, by using the radiometric calibration file recorded by the hyperspectral sensors. It was found that the data values were corrected, as the original data values ranged from 0 to 1,200%, while the data values after the correction ranged from 0 to 100%. It compared the vegetation reflectance of the images corrected with the general vegetation reflectance of trees, to show that a similar reflectance was found to occur at less than 700 ㎚. In addition, the brightness of the images was found to be changed by the visual comparison, after the correction of the back scattering, the radiation, etc. (Figure 9).
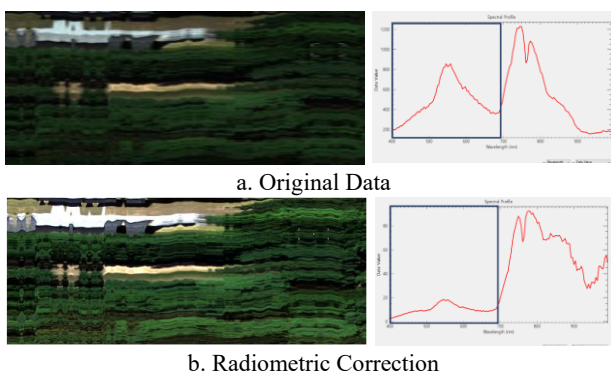

a. Original Data

b. Radiometric Correction

Figure 9. Calibration Result of Unmanned Aerial Hyperspectral

2.5.3   Geometric Correction: The pixels of the images which subjected to the radiometric correction are arranged according to the order of measurement, because the coordinate system is not inputted. Moreover, the positional errors of them may be caused by the irregular positions and postures of drones during the shooting and the tiny positional differences between the drones and the GPS of the hyperspectral sensors. This study, therefore, corrected the geometric errors by inputting the Boresight Calibration posture information of MAV, which was acquired before the shooting, for the manned aerial hyperspectral images(Figure 10). It also performed the slope correction to minimize the shade errors caused by terrain and trees, by referencing to the digital elevation model (DEM). It reviewed the accuracy of the geometric correction for images, by comparing accurate coordinates including buildings or structures, during the correction.
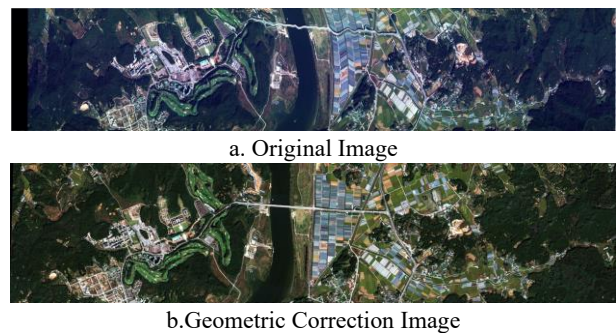

a. Original Image

b.Geometric Correction Image

Figure 10. Calibration Images of Manned Aerial Hyperspectral

After geometric correction with IGM files acquired from UAV hyperspectral images, detailed positional errors were adjusted using Ground Central Point(GCP). It selected 13 points as GCP, which can be aerially identified, such as buildings, roads, etc., and corrected specific positions by using them(Figure 11).

Figure 11. GCP Position of Site

The image length is reduced, as the positions of the images are corrected, after the geometric correction. Many pixels may be missed due to the reduction of the image length, and therefore, the data values may be also changed, so it is necessary to verify such a change(Figure 12).
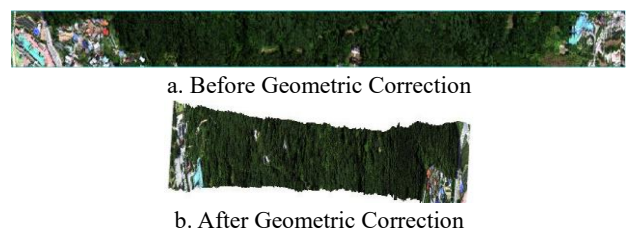

a. Before Geometric Correction

b. After Geometric Correction

Figure 12. Comparison of Unmanned Hyperspectral Images before and after Geometric Correction

The International Archives of the Photogrammetry, Remote Sensing and Spatial Information Sciences, Volume XLVIII-M-2-2023
29th CIPA Symposium "Documenting, Understanding, Preserving Cultural Heritage:
Humanities and Digital Technologies for Shaping the Future", 25–30 June 2023, Florence, Italy

In order to check whether the geometric correction has been performed, it is checked whether the geometric correction has been properly performed by comparing the coordinate values of the RGB image with accurate location information and the data before and after the geometric correction(Figure 13).

The coordinates of buildings, whose positional information is accurately known, were set as the same in the RGB images before and after the correction, and a comparison of the coordinate positions of an image shows that the position of the image was 36°17'20N and 126°55'E before the geometric correction, while it was 36°17'13N, 126°54'54 E after the geometric correction, and the position of the RGB image was 36°17'13N, 126°54'56E, so the coordinate of the starting point was changed, indicating that the starting point was different before the correction, compared to the RGB.

This shows that when the image after geometric correction, in which the existing error has been finely adjusted through geometric correction, is compared with the RGB image, the position and size of the actual building are the same, so the location and size of the geometric correction image have been adjusted.
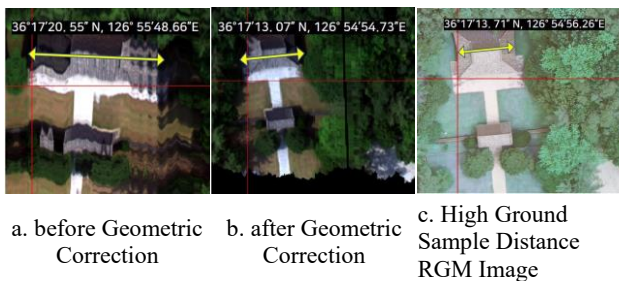

a. before Geometric Correction   b. after Geometric Correction   c. High Ground Sample Distance RGM Image

Figure 13. Comparison of coordinates in the image according to geometric correction

2.5.4   Atmospheric Correction: The atmospheric correction is a process for changing the net surface reflectance, by removing the geometric effect, to acquire the accurate spectral reflection characteristics of the surface objects. In other words, it corrects the atmospheric absorption, scattering and refraction, and aerosol.

It performed the radiation-transfer model-based Atmospheric Correction-4 (ATCOR-4) for the atmospheric correction of manned aerial hyperspectral images by using the MODTRAN-5. ATCOR-4 is optimized for plains and undulated terrains and is generally used for the data acquired by the non-orbital remote sensing(Jensen, 2016). It set the atmospheric modeling data and performed the atmospheric correction, by using the Bidirectional Reflectance Distribution Function(BRDF), a technique for defining the reflectance distribution on an irregular slop and the sun geometric information at the shooting area.

It performed the Quick Atmospheric Correction(QUAC) for the atmospheric correction of the unmanned aerial hyperspectral images, by using ENVI. QUAC uses the shortwave infrared wavelength range for visible rays during the atmospheric correction and is used for both multispectral and hyperspectral images. In addition, it is a model based on empirical results, so it can be applied to different sensors or at the sun altitude. QUAC produces relatively accurate spectral reflection, even when the radiometric correction is not properly performed or there is no information about the solar irradiance because clouds occur(Bernstein et al., 2012).

It was found that the atmospheric correction was properly performed from the unmanned aerial hyperspectral image that subjected to the atmospheric correction, because the spectral graph of general trees was similar to the image at the wavelength of 700 ㎚ after. The figures of trees definitely appear in the image corrected, so some tress could be distinguished(Figure 14).
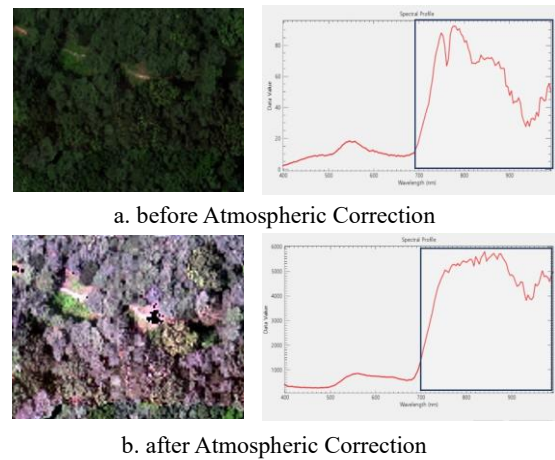

a. before Atmospheric Correction

b. after Atmospheric Correction

Figure 14. Comparison of Unmanned Hyperspectral Image Subjecting to Atmospheric Correction and Spectral Graph

2.5.5   Removal of Mosaic and Noises: It first removed remaining noises from the data by applying the Spectral Polishing of the Savizky–Golay to the manned aerial hyperspectral images (Figure 15).
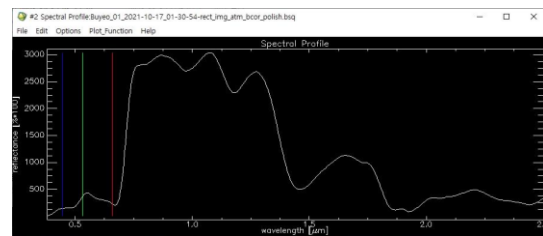

Figure 15. Removal of Manned Hyperspectral Image Noises

It combined the images with the noises removed at each course into a mosaic image (Figure 16), and verified the coordinate of the study site to review the alignment.
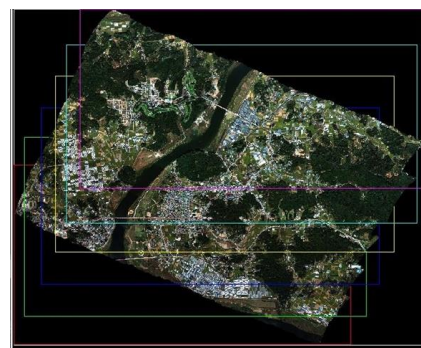

Figure 16. Manned Hyperspectral Image Mosaic

It converted unmanned aerial hyperspectral images into a mosaic image based on the position coordinate existing in the strip image, by using the Quick Mosaic function in the ENVI. Then, it removed unnecessary parts such as roads and buildings from the mosaic image(Figure 17).

Noise occurs in the interval in which the strips meet in the image after the Mosaic, in spite of the pre-processing of it(Figure 18).
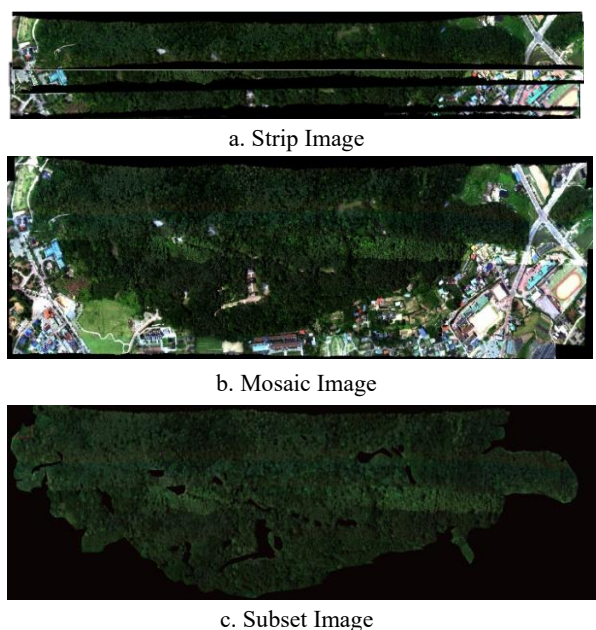
The International Archives of the Photogrammetry, Remote Sensing and Spatial Information Sciences, Volume XLVIII-M-2-2023
29th CIPA Symposium "Documenting, Understanding, Preserving Cultural Heritage:
Humanities and Digital Technologies for Shaping the Future", 25–30 June 2023, Florence, Italy

a. Strip Image

b. Mosaic Image

c. Subset Image

Figure 17. Unmanned Hyperspectral Image Mosaic
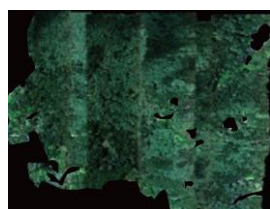
Figure 18. Occurrence of UAV Hyperspectral Image Strip

It was found that there was no problem in the data, by verifying the DN of the junctional boundary in the image, and there was no difference between DN of the image by strips and DN of the mosaic image, so the data has no problem and it was determined that it is possible to conduct an analysis including detection on the image. it is, however, necessary to compensate the images by applying other correction models to them, to increase the quality of them.

2.6 Comparison of Precision

Most of trees growing in the large-area mixed heritage are old and big ones, so the crown width of such a tree amounts to 5-20m. It is, however, impossible to use hyperspectral images in monitoring and diagnosing the natural heritage such as trees, until it becomes possible to distinguish a single old and big tree, and it is necessary acquire the ground sample distance which is high enough to diagnose changes in their growing conditions.
The GSD of the manned aerial hyperspectral image acquired by this study was 150 ㎝/pixel, so it was not possible to clearly distinguish the pixels among the trees and identify the figure of a single tree. The GSD of the unmanned aerial hyperspectral image was 30 ㎝/pixel, so it was possible to identify the figures of individual trees, and moreover, it was also possible to categorize object by their characteristics such as shades and bare land in communities(Table 3).
The findings suggest that the aerial hyperspectral images can be applied in and are useful for monitoring and diagnosing the natural heritage in the large-area mixed heritage.

3. CONCLUSION

This study compared the pre-processing and the precision between MAV- and UAV-borne hyperspectral images. It, therefore, establish how to produce the aerial hyperspectral images with the ground sample distance which is high enough to distinguish individual trees in the large-area mixed heritage.
There were prominent differences in the frequency of the calibration, due to the space errors and the rotation difference between GPS and the hyperspectral sensors in the drones, in collecting the data. It was necessary to perform the slop correction for the manned hyperspectral images by using DEM, different from the unmanned hyperspectral images. In addition, the additional work was required to remove the remaining noises even after the atmospheric correction, because the manned hyperspectral images are greatly influenced by the atmosphere. The unmanned aerial hyperspectral images shot at the low altitude have high ground sample distance enough to distinguish even a single tress, so there was the significant difference in the precision between the unmanned and manned hyperspectral images. This suggests that the unmanned hyperspectral images can be used in monitoring and diagnosing the health of vegetation in the large-area mixed heritage. There were, however, differences between strips in the unmanned hyperspectral images pixelated, so a follow-up study is warranted.

REFERENCES

Bernstein, L.S., X. Jin, B. Gregor, and S.M. AdlerGolden, 2012. The quick atmospheric correction(QUAC) code: algorithm description and recent upgrades, SPIE Optical Engineering, 51(11):111719.

Jensen J. R., 2016. Introductory digital image processing: Remote Sensing Perspective, SigmaPress.

Kim, S.H, Ma, J.R., Kook. M.J., & Lee,K.S., 2005. Current Status of Hyperspectral Remote Sensing: Principle, Data Processing Techniques, and Applications. Korean Journal of Remote Sensing, 21(4), 341−369. https://doi.org/10.7780/KJRS.2005.21.4.341

Kolokoussis, P., Skamantzari, M., Tapinaki, S., Karathanassi, V., & Georgopoulos, A., 2021. 3D and hyperspectral data integration for assessing material degradation in medieval masonry heritage buildings. Int. Arch. Photogramm. Remote Sens. Spat. Inf. Sci, 43, 583-590.

Park, G. R., Lee, G.S., Cho, G.S., 2021. Accuracy evaluation of domestic and foreign land cover spectral libraries using 51(2),169−184. https://doi.org/10.22640/LXSIRI.2021.51.2.169

Park, H.D., 2011. Remote Sensing for Energy Resources, CIR.

868

Category	Manned Aerial Vehicle	Unmanned Aerial Vehicle		
Hyperspectral Sensor	FENIX 1k	Corning MicroHSI		
Altitude(m)	2,200	300	250	200
GSD(m)	1.5	0.3	0.3	0.3
Pixel	367	8403	8405	8409
Image				
Individual Tree Image				

Table 3. Ground sample distance difference between manned aerial hyperspectral and Unmanned aerial hyperspectral images